Electronic Supplementary information

Facile dual doping strategy via carbonization of covalent organic frameworks to prepare hierarchically porous carbon spheres for membrane capacitive deionization

Yuquan Li[a], Xingtao Xu[b], Shujin Hou[a], Jiaqi Ma[a], Ting Lu[a], Jiachen Wang[a,*], Yefeng Yao[a], Likun Pan[a,*]

Shanghai Key Laboratory of Magnetic Resonance,

School of Physics and Materials Science, East China Normal University, Shanghai 200062, China

Materials

1,4-dioxane, mesitylene, NaCl, poly(vinylidene fluoride) (PVDF) and N-methyl-2-pyrrolidinone (NMP) were purchased from Sinopharm Chemical Reagent Co., Ltd. 4-formylphenylboronic acid (FPBA) was purchased from Sigma-Aldrich Chemical Co. 1,3,5-tris(4-aminophenyl)-benzene (TAB) was purchased from ChengDu TongChuangYuan Pharmaceutical Co., Ltd. All reagents were used without further purification.

Experimental Section

Synthesis of TAB-TPBA-COF. The synthesis of TAB-TPBA-COF was conducted according to a procedure reported by Li et al.[1] In brief, a 25 mL thick walled pressure tube was charged with TAB (100 mg, 0.28 mmol), FPBA (100 mg, 0.28 mmol), mesitylene/1,4-dioxane (10 mL, 1/1 by vol.), and the mixture was sonicated for 2 min. After heated at 120 °C for 3 d, the precipitate was collected by centrifugation and washed with 1,4-dioxane. Finally, the obtained yellow powders were dried in a vacuum oven at 80 °C for 24 h.

Synthesis of PCSs. The as-prepared TAB-TPBA-COF were thermally treated in nitrogen for 2 h at a heating rate of 5 °C min^{-1} to obtain PCSs.

Material characterization

^{13}C NMR spectra were recorded on a Bruker Advance III 400WB spectrometer. The surface morphology and structure of samples were examined by field emission scanning electron microscopy (FESEM, JEOL JSM-LV5610) and transmission electron microscopy (TEM, CM200). Thermal gravimetric analysis (TGA) was

conducted on a Shimadzu-50 themoanalyser in N_2 with a heating rate of 10 °C min^{-1} from room temperature to 1000 °C. Raman spectroscopy (DXR, Thermo-Fisher Scientific with a 532nm argon-ion laser), powder X-ray diffraction (XRD, Holland Panalytical PRO PW3040/60 using Cu Kαradiation, λ =1.5418 Å), X-ray photoelectron spectroscopy (XPS, Thermo ESCALAB 250X) were used to analyze the structures of samples. N_2 adsorption/desorption isotherms were measured using an ASAP 2020 Accelerated Surface Area and Porosimetry System (Micrometeritics, Norcross, GA) at 77 K. The specific surface areas of samples were estimated based on the Brunauer-Emmett-Teller (BET) model by using the adsorption branch data in the relative pressure (P/P_0) range of 0.05-0.3. The pore size distribution profile was analyzed on the basis of Barret-Joyner-Halenda (BJH) model.

Electrochemical measurements

For electrode preparation, 80 wt% sample was mixed with 10 wt% carbon black and 10 wt% PVDF in NMP solvent. After homogenously mixed, the carbon slurries were dropped onto graphite paper (thickness: 1 mm) and dried at 60°C for 24 h.

Cyclic voltammetry (CV) and galvanostatic charge-discharge (GCD) were carried out on an electrochemical workstation (AUTO-LAB PGSTAT302 N) in 1 M NaCl solution in a three-electrode mode, including a standard calomel electrode as reference electrode and a platinum foil as counter electrode.

Specific capacitance C (F g^{-1}) was calculated from GCD curves according to the following equation:

$$C = \frac{I \times \Delta t}{m \times \Delta V}$$

where I is the current (A), Δt is the time (s), m is the mass of active materials (g) and ΔV is the voltage window (V).

Batch-mode electrosorption tests

To study the electrosorption performance, PCSs were mixed with carbon black and PVDF (8:1:1 weight ratio). The mixture was coated on graphite paper and dried in oven at 60 °C overnight. The area and mass of each electrode were 32 cm^2 and ~70 mg, respectively. MCDI and CDI experiments were conducted in a continuously recycling system, as described in our previous work.[2] Analytical pure NaCl solution was employed as target solution. The solution volume and flow rate were 100 mL and 50 mL min^{-1}, respectively. A direct voltage was applied onto electrodes. The concentration variation was continuously monitored and measured at the outlet of unit cell by using an ion conductivity meter. The relationship between conductivity and concentration was obtained according to a calibration table made prior to the experiment.[2] Salt adsorption capacity (SAC) (mg g^{-1}) was calculated as the following[3]:

$$SAC = \frac{(C_f - C_0) \times V}{M}$$

where C_f and C_0 are final and initial NaCl concentrations (mg L^{-1}), V is the solution volume (L) and M is total mass of electrodes (g). The charge efficiency (Λ) is used to determine the effectiveness of electrical double layer on storing salt ions and given as[4]:

$$\Lambda = \frac{SAC \times F}{58.44 \times 1000 \times \Sigma}$$

where Σ is specific charge (C g^{-1}) and F is the Faraday's constant of 96485 (C mol^{-1}). The salt adsorption rate (SAR) is calculated as following:

$$SAR = \frac{SAC}{t}$$

where t stands for electroadsorption time.

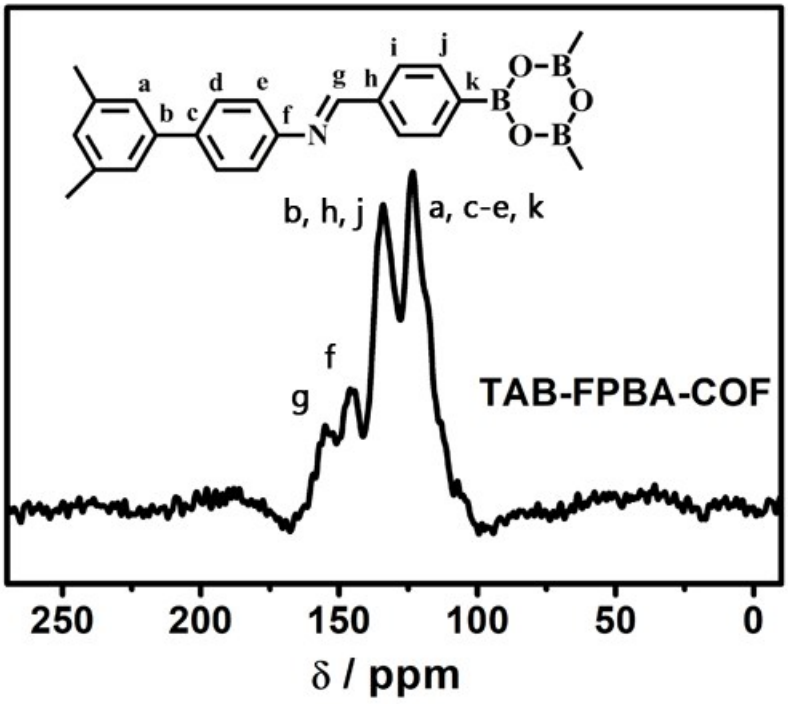

Fig. S1 TGA curve of TAB-FPBA-COF.

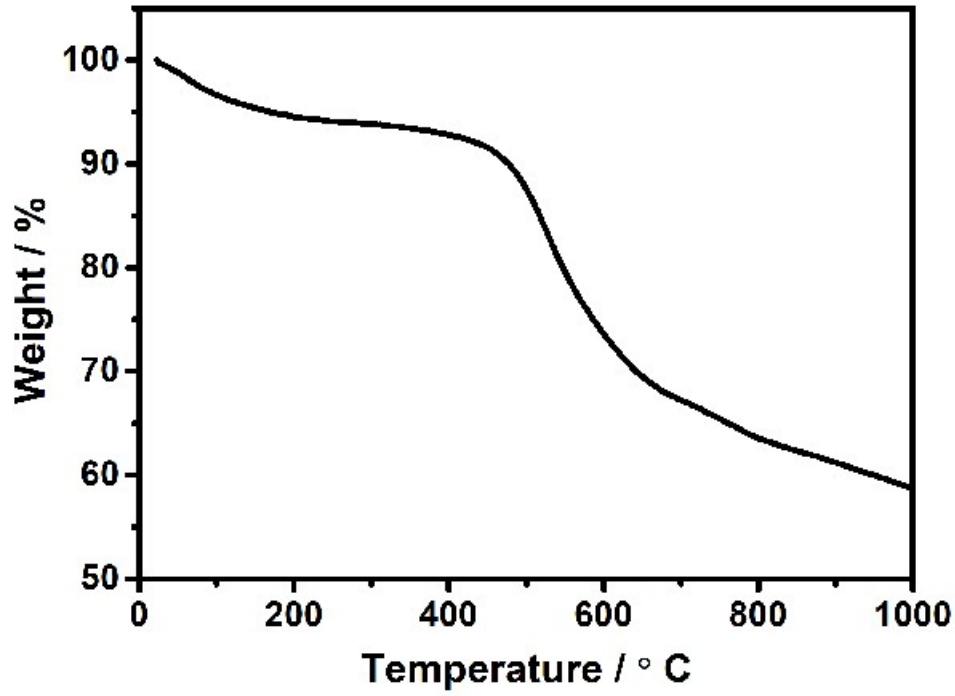

Fig. S2 Solid state ^{13}C NMR for TAB-FPBA-COF.

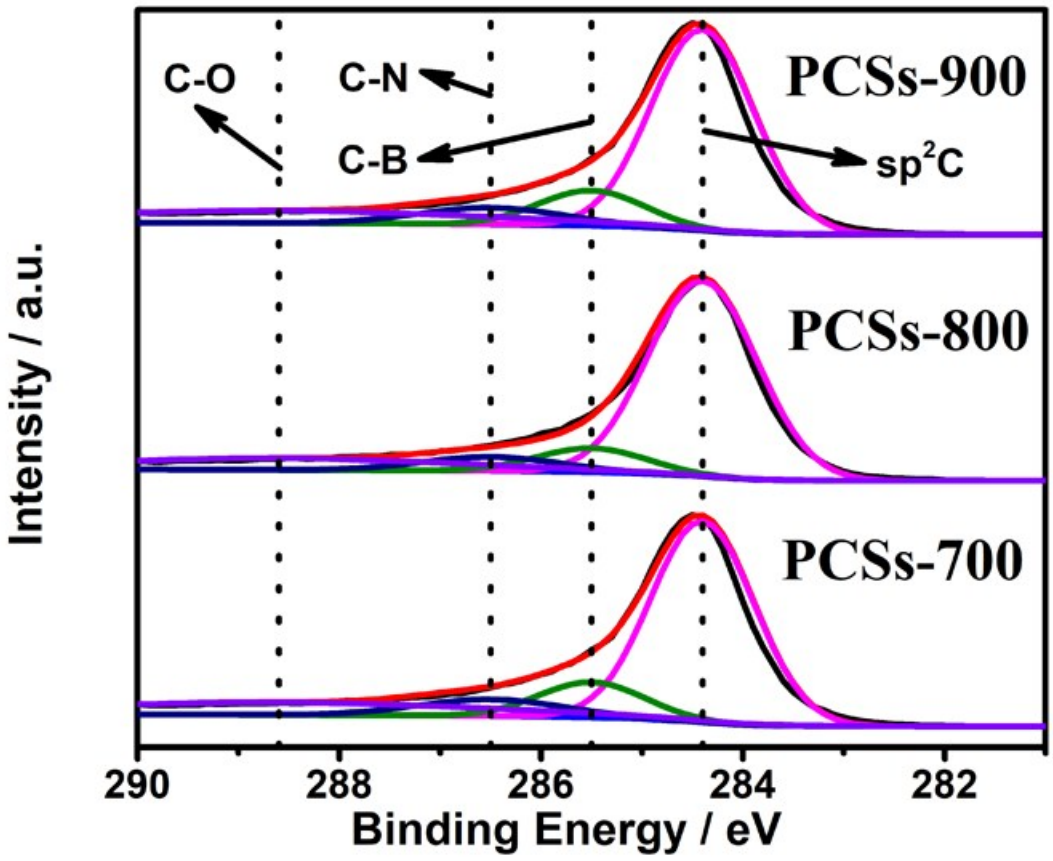

Fig. S3 High-resolution XPS C1s spectra of PCSs

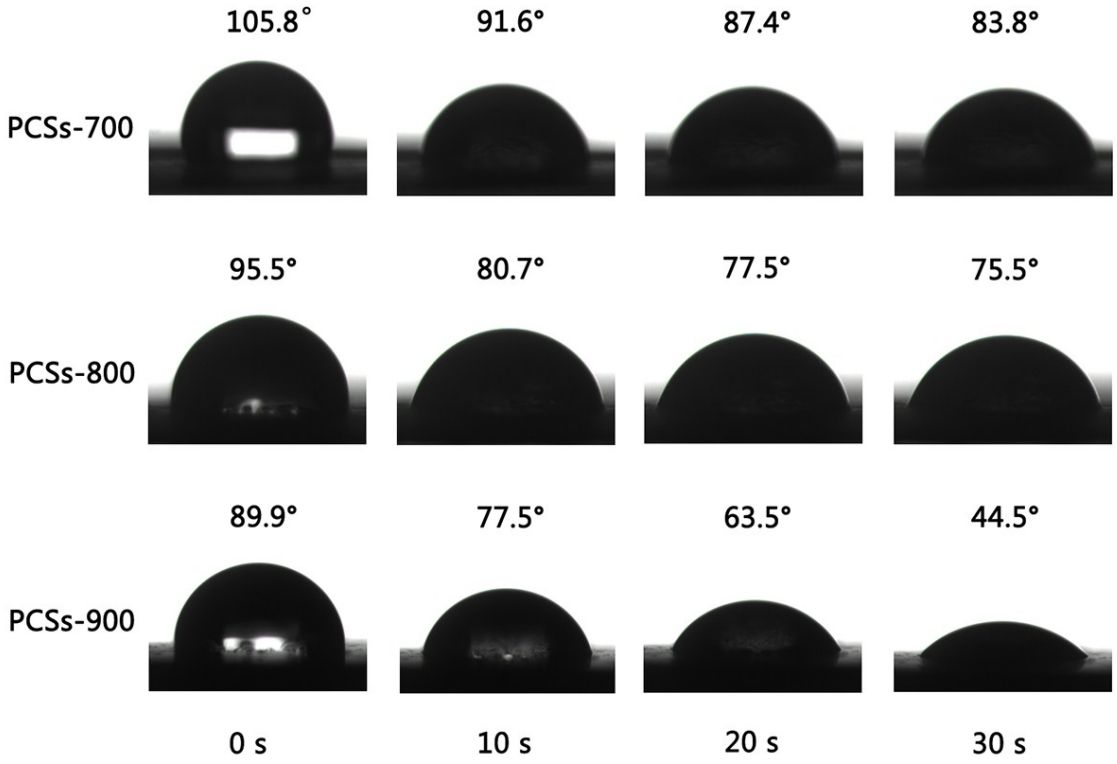

Fig. S4 Optical micrographs of water contact angle of PCSs electrode at different time.

Table S1 Elemental contents (at. %) in PCSs from XPS analysis.

Sample	C	N	B
PCSs-700	93.62%	3.94%	2.44%
PCSs-800	92.66%	3.95%	3.39%
PCSs-900	91.64%	3.8%	4.56%

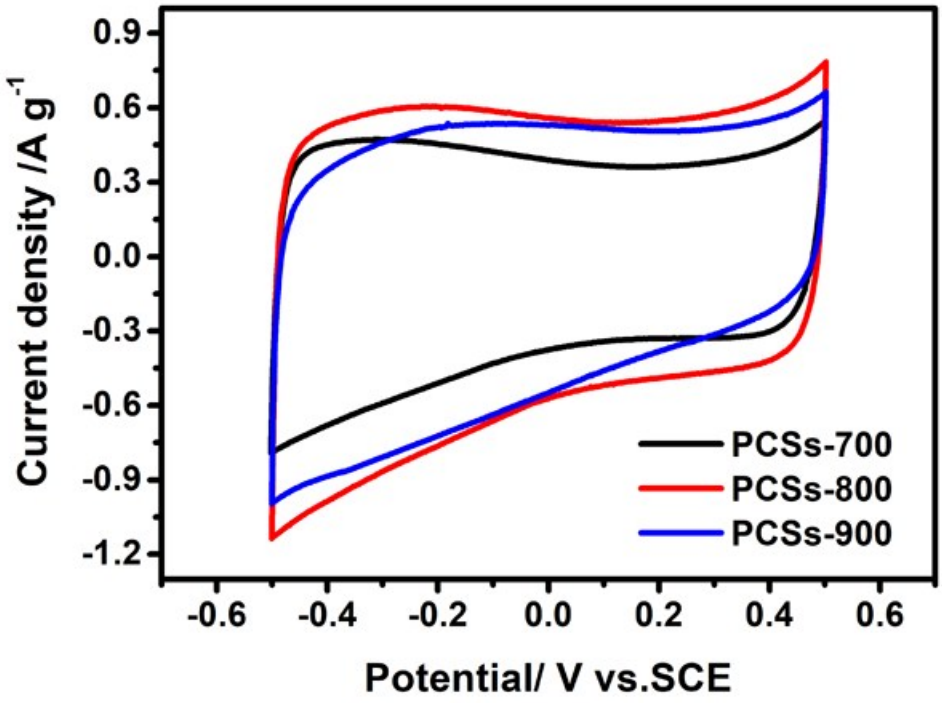

Fig. S5 CV curves of PCSs at 1 mV s^{-1}.

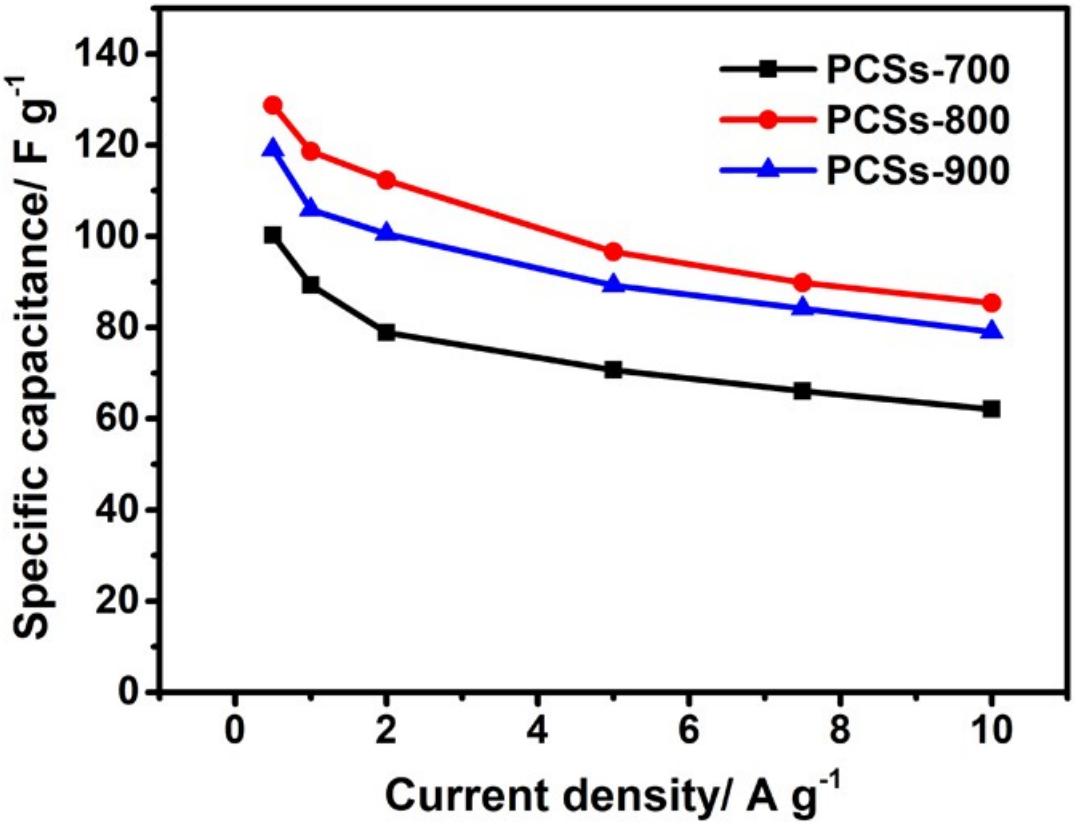

Fig. S6 Specific capacitance of PCSs at different current densities.

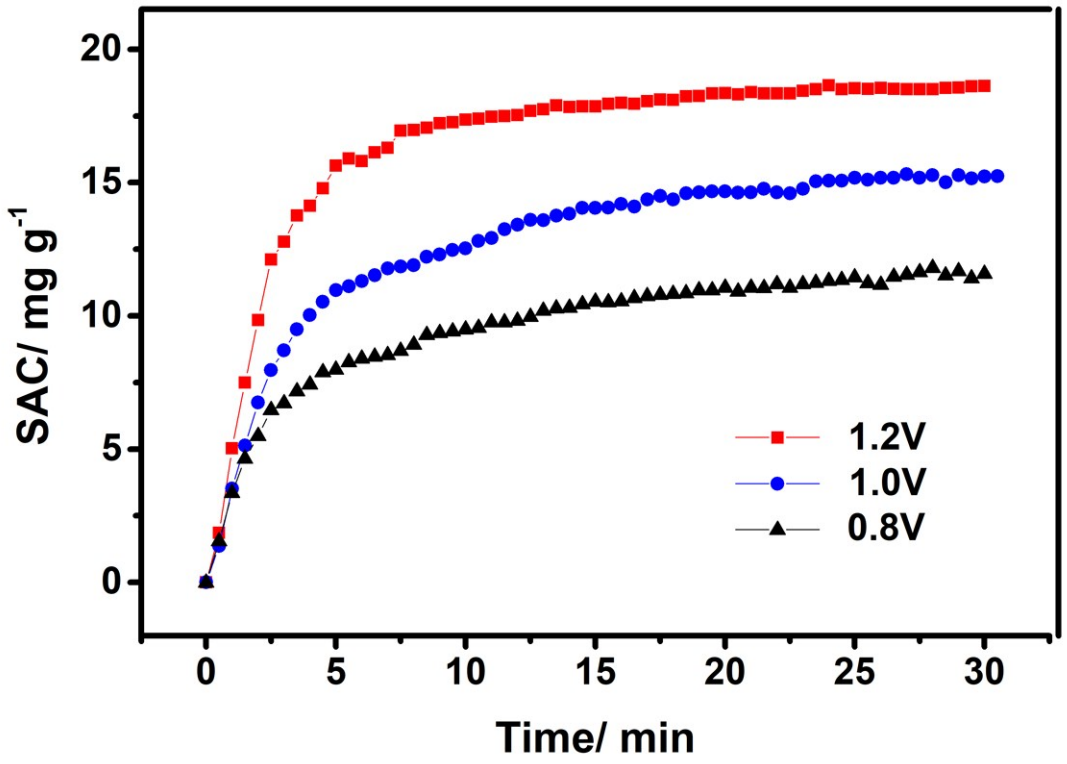

Fig. S7 CDI performances of PCSs-800 in 500 mg L^{-1} NaCl solution at different cell voltages.

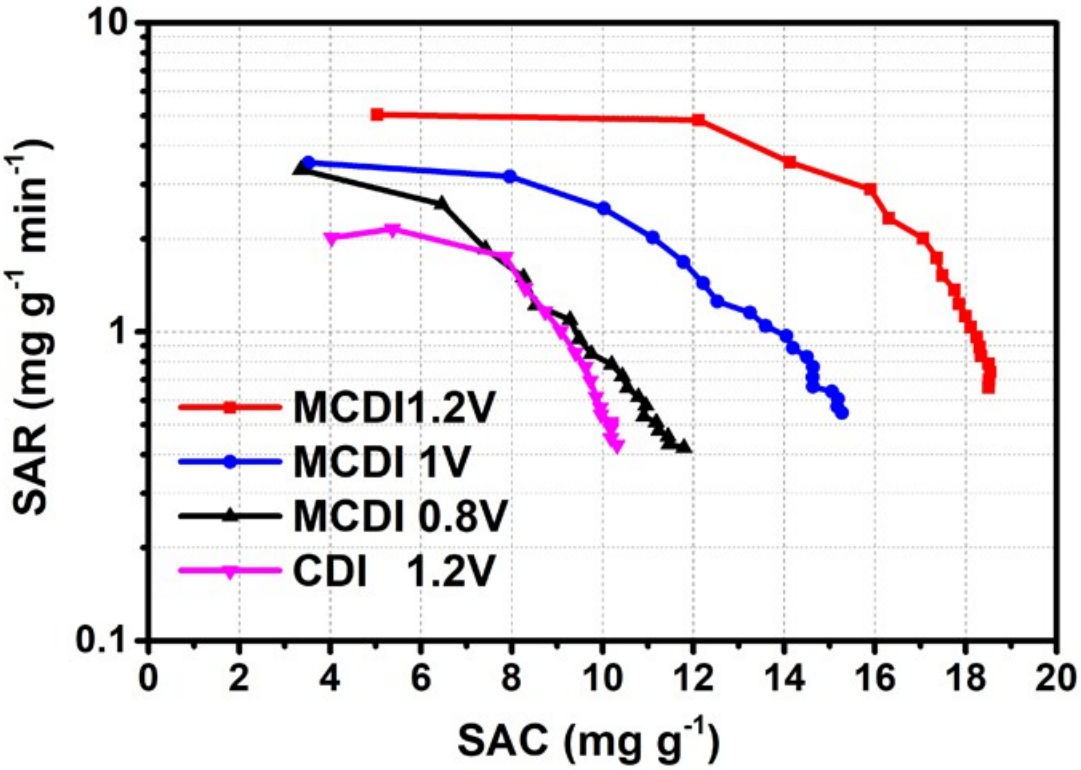

Fig. S8 Ragone plot of SAR vs SAC of PCSs-800.

Table S2 Comparison of SAC between PCSs-800 in this work and various carbon materials that were prepared via activator-free process reported in the literatures.

Electrode material	Applied voltage (V)	Initial NaCl concentration (mg L^{-1})	SAC (mg g^{-1})
Carbon aerogel[5]	1.2	500	2.9
Hollow carbon nanofibers[6]	1.2	45	1.9
Reduced graphene oxide[7]	1.8	~50	3.6
Carbon nanotube sponge[8]	1.2	~60	4.3
Carbon spheres[9]	1.2	500	5.8
3D graphene[10]	1.5	~50	5.0

3D graphene/ TiO_2[11]	1.2	500	9.9
Porous carbon nanofibers[12]	1.2	500	8.1
Porous carbon polyhedra[13]	1.2	500	13.8
PCSs-800 (CDI)	1.2	500	10.3
PCSs-800 (MCDI)	1.2	500	18.5

References:

1. L. Li, L. Li, C. Cui, H. Fan and R. Wang, *ChemSusChem*, 2017, **10**, 4921-4926.
2. H. Li, L. Pan, C. Nie, Y. Liu and Z. Sun, *J. Mater. Chem.*, 2012, **22**, 15556-15561.
3. X. Xu, Z. Sun, D. H. Chua and L. Pan, *Sc. Rep.*, 2015, **5**, 11225.
4. R. Zhao, P. Biesheuvel, H. Miedema, H. Bruning and A. Van der Wal, *J. Phys. Chem. Lett.*, 2009, **1**, 205-210.
5. J. C. Farmer, D. V. Fix, G. V. Mack, R. W. Pekala and J. F. Poco, *J. Electrochem. Soc.*, 1996, **143**, 159-169.
6. A. G. El-Deen, N. A. M. Barakat, K. A. Khalil and H. Y. Kim, *New J. Chem.*, 2014, **38**, 198-205.
7. X. Xu, L. Pan, Y. Liu, T. Lu and Z. Sun, *J. Colloid Interf. Sci.*, 2015, **445**, 143-150.
8. L. Wang, M. Wang, Z.-H. Huang, T. Cui, X. Gui, F. Kang, K. Wang and D. Wu, *J. Mater. Chem.*, 2011, **21**, 18295.
9. Y. Liu, L. Pan, T. Chen, X. Xu, T. Lu, Z. Sun and D. H. C. Chua, *Electrochim. Acta*, 2015, **151**, 489-496.
10. Z.-Y. Yang, L.-J. Jin, G.-Q. Lu, Q.-Q. Xiao, Y.-X. Zhang, L. Jing, X.-X. Zhang, Y.-M. Yan and K.-N. Sun, *Adv. Funct. Mater.*, 2014, **24**, 3917-3925.
11. H. Yin, S. Zhao, J. Wan, H. Tang, L. Chang, L. He, H. Zhao, Y. Gao and Z. Tang, *Adv. Mater.* 2013, **25**, 6270-6276.
12. H. Pan, J. Yang, S. Wang, Z. Xiong, W. Cai and J. Liu, *J. Mater. Chem. A*, 2015, **3**, 13827-13834.
13. Y. Liu, X. Xu, M. Wang, T. Lu, Z. Sun and L. Pan, *Chem. Commun.*, 2015, **51**, 12020-12023.